International Journal of Biological Macromolecules 281 (2024) 136313

Contents lists available at ScienceDirect

International Journal of Biological Macromolecules

journal homepage: www.elsevier.com/locate/ijbiomac

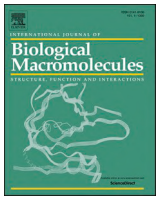

Methacrylated chitosan/jellyfish collagen membranes as cell instructive platforms for liver tissue engineering

Sabrina Morelli [a,*,1], Ugo D'Amora [b,1], Antonella Piscioneri [a], Maria Oliviero [b], Stefania Scialla [b], Alessandro Coppola [c], Donatella De Pascale [c], Fabio Crocetta [d,e], Maria Penelope De Santo [f], Mariano Davoli [g], Daniela Coppola [c,*], Loredana De Bartolo [a]

[a] Institute on Membrane Technology, National Research Council of Italy, CNR-ITM, Via P. Bucci, Cubo 17/C, I-87036 Rende, (CS), Italy
[b] Institute of Polymers, Composites and Biomaterials, National Research Council, CNR-IPCB, Naples, Italy
[c] Ecosustainable Marine Biotechnology Department, Stazione Zoologica Anton Dohrn, Via Acton 55, 80133 Naples, Italy
[d] Integrative Marine Ecology Department, Stazione Zoologica Anton Dohrn, Villa Comunale, 80121 Naples, Italy
[e] NBFC, National Biodiversity Future Center, Palermo Piazza Marina 61, 90133 Palermo, Italy
[f] Department of Physics and CNR-Nanotec, University of Calabria, Rende, (CS), Italy
[g] Department of Biology, Ecology and Earth Science, DiBEST, University of Calabria, Rende, (CS), Italy

ARTICLE INFO

Keywords:
Methacrylated chitosan
Marine collagen
Polymeric membranes
Liver tissue engineering

ABSTRACT

Although the multidisciplinary area of liver tissue engineering is in continuous progress, research in this field is still focused on developing an ideal liver tissue template. Innovative strategies are required to improve membrane stability and bioactivity.

In our study, sustainable biomimetic membranes were developed by blending methacrylated chitosan (CSMA) with jellyfish collagen (jCol) for liver tissue engineering applications.

The *in vitro* biological behaviour demonstrated the capability of the developed membranes to create a suitable *milieu* to enable hepatocyte growth and differentiation. The functionalization of chitosan together with the biocompatibility of marine collagen and the intrinsic membrane properties offered the ideal biochemical, topographical, and mechanical cues to the cells. Thanks to the enhanced CSMA/jCol membranes' characteristics, hepatocytes on such biomaterials exhibited improved growth, viability, and active liver-specific functions when compared to the cell fate achieved on CSMA membranes. Our study provides new insights about the influence of membrane properties on liver cells behaviour for the design of novel instructive biomaterials. The enrichment of functionalized chitosan with marine collagen represents a promising and innovative approach for the development of an appropriate platform for hepatic tissue engineering.

1. Introduction

The creation of biomimetic materials for the regeneration and repair of injured tissues and organs remains a challenging issue in biomedical field. Specially, the regulation of specific biomaterial characteristics in the development of ideal tissue and/or organ analogues and their bioactivation through signals, capable of directing cell and tissue fate, represent a crucial challenge in tissue engineering. Membrane-based approaches are successfully employed for the creation of various functional tissue-engineered constructs [1–3]. Polymeric membranes are suitable material for liver tissue engineering owing to their intrinsic characteristics of high selectivity and permeability together with their ability to be easily scaled-up with modulated structural, physicochemical and mechanical properties. It is widely recognized that membranes offer specific cues to hepatocytes for recapitulating the in vivo *milieu* of natural microenvironments, driving three-dimensional (3D) liver tissue formation [4–6]. However, concerted efforts towards innovative strategies and approaches are still needed to improve membrane performance in terms of stability and bioactivity aiming at developing an ideal functional liver tissue for biomedical applications. Natural polymers, such as collagen, and chitosan (CS), exhibit several attractive features for the hepatic tissue regeneration. Their combination offers at the

* Corresponding authors.
E-mail addresses: s.morelli@itm.cnr.it, sabrina.morelli@cnr.it (S. Morelli), daniela.coppola@szn.it (D. Coppola).
[1] These authors contributed equally

https://doi.org/10.1016/j.ijbiomac.2024.136313
Received 29 April 2024; Received in revised form 17 July 2024; Accepted 3 October 2024
Available online 5 October 2024

cellular interface a proper microenvironment that resembles the natural liver niche. CS is the most common naturally occurring cationic polymer that comes from the *N*-deacetylation of chitin, the second most prevalent biopolymer found in nature. CS has a large number of uses in tissue engineering due to its own features like biodegradability, nontoxicity and biocompatibility. It has a structural similarity to glycosaminoglycans, which are components of the liver extra cellular matrix (ECM), making it an efficient biomaterial for liver tissue engineering [7]. Nevertheless, CS must be modified to balance its hydrophilic character and poor stability before it can be potentially used in tissue engineering. These modifications can be effectively achieved in CS considering that it has many functional groups, including hydroxyl (OH) and amino (NH_2) groups. Hence, its structure can be precisely controlled by physically or chemically crosslinking of the polymer chains. Both strategies show peculiar drawbacks and limitations. Indeed, physical crosslinking does not allow obtaining biomaterials with appropriate structural stability, in high or low pH environments, and controlled biodegradation rates. On the other side, chemically crosslinking is potentially cytotoxic, due to possible presence of unreacted reagents entrapped in the system. Furthermore, it is widely reported that common crosslinkers, such as formaldehyde and glutaraldehyde, are not cell friendly. To overcome these disadvantages, and to produce strong and durable biomaterials, photocrosslinking has emerged as an alternative chemical crosslinking approach in which chemically modified polymer derivatives, such as methacrylated chitosan (CSMA), without using hazardous chemical crosslinkers, are employed [8]. Moreover, the functionalization reaction can occur quickly, at room temperature, and physiological pH [9].

In this work, the idea was to functionalize CS with methacrylic anhydride (MA), obtaining a CSMA polymer that could be photocrosslinked by activating the carbon–carbon double bond using Irgacure 2959 as an initiator to create a free radical under ultraviolet (UV) light. The aim was to improve the stability and better tune the degradation time, providing a more cohesive and stable material. Furthermore, in the recent years, polymer blending is one of the most successful methods for providing suitable polymeric materials with desirable properties for specific tissue engineering applications. Many polymers have been used to improve the properties of CS-based biomaterials. Among them, collagen is particularly interesting as it represents the main structural component of the ECM in all connective tissues and interstitial tissues of the parenchymal organs. Collagen has excellent mechanical strength and viscoelasticity, which allow it to be involved in several biological activities of the human body, such as cell proliferation, migration, and adhesion. This biomaterial has attracted the interest of researchers as it has excellent biocompatibility, low antigenicity, biodegradability, hydrophilicity, and cell adhesive properties for soft tissue engineering applications. Recently, marine organisms have drawn attention as biocompatible, eco-friendly, and safe sources of collagen. Marine collagen removes the risk of transmissible diseases, overcomes the limits of religion and, at the same time, exhibits high similarity in morphology and function with mammal collagen [10]. The growing attention to possible uses of fishing discards, including fishing by-catch as jellyfish, plays an important role in economic growth and sustainable development, as they represent a rich and eco-friendly source of value-added compounds [11]. Many studies have shown that the jellyfish organic matter consists mainly of collagen [12]. Among different species already studied, the scyphomedusan *Rhizostoma pulmo* from the Mediterranean Sea presents high collagen content compared to other jellyfish [13]. Furthermore, the increase in water temperature as a result of global climate change causes seasonal blooms resulting both in direct and indirect negative impacts and an increase in plentiful supply. Studies obtained so far on jellyfish collagen have shown that it exhibits greater cell viability to osteoblasts and fibroblasts compared to other biomaterials, including bovine collagen, as reported by Song et al. [14], probably due to some differences in their amino acid composition. Furthermore, it displays low antigenicity and intrinsic ability to trigger immune reaction in <1 % of the general population [15].

Jellyfish collagen (jCol) was extracted from *R. pulmo* obtained from fishery by-catch, to establish a sustainable process in line with the zero-waste and circular economy procedures. Previous studies have shown that the *R. pulmo* collagen shows a high degree of similarity to the mammalian type I collagen [16] and shares important characteristics with it, such us the ability to support two dimensional (2D) and 3D cell cultures.

Taking advantage of the properties of each compound, namely CSMA and jCol, and to reduce specific limitations of each single material, such as poor mechanical stability, inappropriate degradation rate and wettability, we explored new sustainable bioactive composite membranes for the creation of an in vitro liver tissue analogue. A CSMA membrane and two blend membranes with different percentages of polymers were prepared by phase inversion technique. The membranes were fully characterized to assess their morphology, roughness, wettability, biodegradation, and mechanical properties, which play an important role in guiding hepatocyte differentiation and maintenance of specific functions.

The effects of the different composition-related properties of the developed membranes were analysed on liver cell behaviour by culturing embryonic liver cells up to 18 days. Within the membrane systems cell morphology, viability and functional hepatic differentiation were analysed; albumin production, glycogen storage, and expression of liver specific markers were assessed to address how changes in membrane composition could affect membrane properties, which strongly influence hepatic growth and differentiation. We investigated the role of marine collagen in dictating membrane characteristics and its efficiency in inducing liver tissue regeneration with the final goal to demonstrate the potential of these sustainable biomimetic membranes as new generation of membranes with excellent comprehensive performance.

Research on membranes developed by the enrichment of CSMA with marine collagen to provide suitable hepatic tissue microenvironment for functional hepatocytes is still ongoing. Thus, our research establishes new perspectives in this field. Furthermore, the main novelty of the work is that, for the first time, two techniques—solvent casting for the synthesis of membranes, and photocrosslinking—were coupled as a promising and innovative approach for the creation of novel instructive biomaterials for liver tissue engineering applications.

2. Materials and methods

2.1. Raw material collection

Jellyfish were obtained from the by-catch of commercial fishing activities held in the marinas of Monte di Procida and Mondragone (central-western Mediterranean Sea). In particular, *Rhizostoma pulmo* (Macri, 1778) specimens were collected in September 2021 and June 2022 using trammel nets (1 m in height and ~ 550 m in length; net consisting of an inner panel of 4.8 cm stretched mesh between two panels of 25 cm stretched mesh) fishing passively on a sandy bottom off the Fusaro Lake mouth (40.8230° N, 14.0451° E) and off the Agnena river mouth (41.0743° N, 13.8988° E). Soon after disentangling them from nets, jellyfish were placed into cold storage containers in single plastic bags filled with seawater, and soon transferred to the Laboratory of Benthos-Napoli (Stazione Zoologica Anton Dohrn, Naples, Italy) for subsequent laboratory work.

2.2. Collagen extraction and characterization

All steps of the acid-soluble collagen extraction were carried out on fresh jellyfish, at 4 °C, according to the method described by Addad and collaborators [16], with slight modifications. Briefly, the umbrella and oral arms of each specimen were separated to perform the extraction separately and cut into small pieces. To remove non-collagenous proteins, jellyfish pieces were washed with distilled water and soaked in 0.1 M sodium hydroxide (NaOH, Sigma Aldrich, Milan, Italy) with a wet

tissue/solution ratio of 1:1 (*w/v*) overnight, under continuous stirring. The treated tissues were washed with distilled water until neutral pH was reached and then extracted with 0.5 M acetic acid (CH_3COOH, Sigma Aldrich, Milan, Italy) (1:1 w/v) and stirred for 3 days, twice. The insoluble components were separated with cotton cloth and the filtrates were centrifuged at 20000 x*g* for 1 h. The acid-soluble collagen was precipitated by adding sodium chloride (NaCl, Sigma Aldrich, Milan, Italy) to a final concentration of 0.9 M. The precipitate was collected by centrifugation at 4 °C, 20000 x*g* for 1 h. The pellet was dissolved in a minimum volume of 0.5 M CH_3COOH, and dialyzed against 0.1 M CH_3COOH first, subsequently against distilled water, then lyophilised for subsequent uses.

Sodium Dodecyl Sulphate - PolyAcrylamide Gel Electrophoresis (SDS–PAGE) was performed by the method of Laemmli, with modifications. 1 mg of jCol was dissolved in 100 μL of CH_3COOH, then mixed with 100 μL Tris (hydroxymethyl) aminomethane (THAM) hydrochloride (Tris–HCl, Sigma Aldrich, Milan, Italy), pH 8.8 containing 4 % SDS. The samples were heated at 50 °C for 5 min. Solubilized samples were mixed with the sample buffer 2× (0.5 M Tris–HCl, pH 6.8, 5 % SDS, 20 % glycerol, 10 % 2-mercaptoethanol) and 10 μL of each sample were loaded onto a polyacrylamide gel (7.5 % separating gel and 4 % stacking gel) and subjected to electrophoresis, at 140 *V*. Coomassie Brilliant Blue R-250 was used for the visualization of the bands. Spectra Multicolor High Range Protein Ladder (Thermo Fisher Scientific, MA, United States) was used as protein marker and the type I collagen from Calf skin (Sigma Aldrich, MA, United States) was used as standard.

Fourier-transform infrared (FTIR) spectroscopy in attenuated total reflectance (ATR) mode, using lyophilized jCol samples, was performed (Thermo Fisher Nicolet IS10, Waltham, MA, United States of America) between 4500 and 500 cm^{-1} with a resolution of 2 cm^{-1}, with each spectrum being the average of 32 scans, to evaluate the presence of collagen's characteristic chemical bounds/groups.

X-Ray diffraction analysis (XRD) was exploited to examine the crystal structure of extracted jCol. The lyophilized jCol sample was scanned using an XRD instrument (XPERT-PRO, Malvern Panalytical, United Kingdom) with Cu Kα radiation (λ = 1.54060 Å). Voltage and current were fixed at 40 kV and 30 mA, respectively. The scanning range was set to be between 10° and 80° (2θ) in a fixed time mode at room temperature, meanwhile voltage and current were 0 kV and 30 mA, respectively.

2.3. CSMA synthesis and characterization

CSMA was synthesized according to literature with minor modifications [8]. Briefly, high molecular weight CS (1.5 g) (HM_wCS, M_w - 310,000-375,000 Da, degree of deacetylation >75 %, Sigma Aldrich, Milan, Italy) was first dissolved in 4%*v*/v CH_3COOH (100 mL) overnight at 40 °C under magnetic stirring. 4.6 mol methacrylic anhydride (MA, Sigma Aldrich, Milan, Italy) per mole of CS repeat unit, which is equivalent to 6 mL, were slowly added to the solution. The mixture was maintained at 40 °C, under magnetic stirring, for 12 h, protected from light. Afterwards, the products were redispersed in deionized water (for chromatography LC-MS Grade, conductance at 25 °C ≤ 1 μS/cm, Sigma Aldrich, Milan, Italy), purified by dialysis against distilled water for five days, using dialysis membrane tubes (12–14 kDa molecular weight cut-off; Sigma Aldrich, Milan, Italy) to ensure complete removal of MA and CH_3COOH. During the dialysis, distilled water was refreshed at least twice a day. The material was lyophilized (LaboGene's CoolSafe 55–4 PRO, Bjarkesvej, Denmark) and stored at −80 °C for further use.

^1H Nuclear magnetic resonance (^1H NMR, Bruker AVIII 400HD, Fällanden, Swiss) was employed to evaluate the functionalization reaction's effectiveness. CS and CSMA (5 mg/mL) were completely dissolved in deuterium oxide (D_2O) acidified with 30 μL trifluoroacetic acid (Sigma Aldrich, Milan, Italy) and allowed to be dissolved overnight at room temperature using a vortex mixer. Afterwards, they were transferred into NMR tubes and analysed at a frequency of 400 MHz. Phase and baseline corrections were applied before elaborating data.

ATR-FTIR spectroscopy was employed to assess the CS functionalization postmethacrylation reaction. CS and CSMA were scanned between 500 and 4500 cm^{-1} with a resolution of 2 cm^{-1}. Data were analysed on the base of the average of six scans per spectrum.

2.4. Preparation of CSMA/jCol membranes

Membranes were prepared in flat configuration by the inverse phase technique. To obtain the membranes, 2 % *w/v* CSMA was dissolved in a CH_3COOH solution (1 M). Polyethylene glycol (PEG, MW 6000 Da; Merck, Italy) at a 4:1 ratio, and Irgacure 2959 (Sigma Aldrich, Milan, Italy) (5 % w/w_{CSMA}) were added to the CSMA solution, as porogen and photocrosslinker, respectively.

Similarly, CSMA/jCol composite membranes were obtained by varying collagen content into the CSMA solution. Briefly, jCol was dissolved in CH_3COOH (0.5 N) to give a final concentration of 2 mg/mL. The collagen solution was added to the CSMA solution, prepared as described above, by mechanical stirring until a good collagen dispersion was obtained. The collagen content was adjusted to the desired percentage. Two blend membranes with different volume percentages (% *v*/v) of polymers, namely 70 % CSMA and 30 % jCol (CSMA/jCol30), and 50 % CSMA and 50 % jCol (CSMA/jCol50) were produced by mixing the corresponding polymeric solutions. The CSMA and CSMA/jCol solutions with different collagen concentration were cast into a petri dish (Ø =90 mm) and dried at room temperature, until complete solvent evaporation. The membranes were neutralized by immersion in a 1 % NaOH solution, and then washed with distilled water.

All membranes were photocrosslinked by using UV-KUB 2 system (λ: 365 nm, P: 1 J/cm^2) (Kloe, France). Lastly, the membranes were sterilized using UV light in a laminar flow chamber for 30 min.

2.5. Characterization of membranes

The morphology of membranes coated with graphite was examined using a High-Resolution Scanning Electron Microscope (HRSEM mod CrossBeam 350 ZEISS – Germany) @ 5 K*V*olt of energy. Images were acquired with secondary electron signal (SE).

The surface topography was characterized by atomic force microscopy (AFM) using a Multimode VIII equipped with a Nanoscope V controller (Bruker, Santa Barbara, CA, United States). The microscope was operated in tapping mode in air using a lever oscillating at a frequency of 150 kHz (Bruker). Images were acquired on 2 × 2 μm^2 areas, with 256 × 256 acquisition points and a scan rate of 1 Hz. Surface roughness was estimated with respect to the average roughness (Ra) and the root mean squared roughness (Rq).

The chemical composition of membranes was characterized by ATR-FTIR analysis. Infrared spectra were collected using Perkin Elmer Spectrum 100 spectrophotometer (Waltham, USA) in the range of 4000–650 cm^{-1} and with a resolution of 4 cm^{-1}.

Membrane thickness was measured with a micrometer (Carl Mahr 40E, Germany). A capillary flow porometer (CFP 1500 AEXL, Porous Materials Inc., PMI, Ithaca, NY, United States) was employed to measure the mean pore diameter of each membrane.

The wettability of the membranes was determined by water contact angle (WCA) measurements with a contact angle meter (KSV Instruments, Ltd., Helsinki, Finland) by using the sessile drop method. The WCA results are the mean of 30 measurements.

The mechanical properties of membranes were assessed using a tensile testing machine (Zwick/Roell Z2.5, Germany). Five samples of each kind of membrane (4 cm × 1 cm) were analysed under uniaxial tension until failure to determine values of Young's modulus (E), ultimate tensile strength (UTS) and elongation at break (ε).

To assess the degradation properties, the membrane samples (2 cm^2) were placed into phosphate buffer solution (PBS, Sigma Aldrich, Milan, Italy), pH = 7.4, containing lysozyme (1 mg/mL, Sigma Aldrich, Milan,

Italy), supplemented with 0.02 % sodium azide (NaN_3, Sigma Aldrich, Milan, Italy), and incubated at 37 °C. Fresh solution was replaced every 6 days. After regular intervals of time, the samples were removed from the enzymatic solution, washed with distilled water, and dried at 37 °C until reaching constant weight. Then, the dissolution index was calculated as:

$$\%S = \frac{W_i - W_d}{W_i} \times 100 \quad (1)$$

where W_i is the sample weight before incubation in enzymatic solution and W_d is the dried sample weight after dissolution test. Three samples of the developed membranes were characterized and the data were presented as average ± SD.

2.6. Liver cell cultures

Rat embryonic liver cells (17 day embryonic liver of Japanese albino rat) (RLC-18), DSMZ, Braunschweig, Germany) were cultured in RPMI medium containing L-glutamine, supplemented with 10 % (*v*/v) heat-inactivated fetal calf serum (FCS, Euroclone, Milan, Italy) and 100 mg/mL penicillin-streptomycin (Sigma Aldrich, Milan, Italy) at 37 °C in a humidified CO_2 incubator (95 % air, 5 % CO_2) and subcultured twice a week using trypsin (0.05 %)/ Ethylenediaminetetraacetic acid (0.025 %) solution (EDTA, Sigma Aldrich, Milan, Italy). The cells were seeded at 9 passages on the different kind of membranes at a density of 1×10^4 cell/cm^2. The culture medium was changed every 48 h.

2.7. Scanning electron microscopy analysis

The morphology of cells cultured on the developed membranes was analized by SEM observation. At day in vitro (DIV) 14, samples were fixed using 3 % *v*/v glutaraldehyde (Sigma Aldrich, Milan, Italy) with 1 % v/v formaldehyde (Sigma Aldrich, Milan, Italy) in PBS for 30 min at 4 °C, then stained with 1 % v/v osmium tetroxide (OsO_4, Sigma Aldrich, Milan, Italy) in PBS for 30 min at 4 °C, rinsed three times with PBS and dehydrated with a graded series of ethanol (10–100 % *v*/v), and left at room temperature to dry.

2.8. Cell viability

Cell viability was evaluated by trypan blue exclusion test. After 7, 13 and 18 days of culture, cells were detached from the different membrane systems by trypsin/EDTA solution (Euroclone, Italy) treatment and centrifuged at approximately 600 x*g* for 5 min at room temperature. The cell pellet was resuspended in culture media and the total number of cells was determined using trypan blue stain (Sigma Aldrich, Milan, Italy) and hemocytometer under a Light Optic Microscope (Axio Vert, Zeiss, Gemany). Cell viability was calculated as the number of viable cells per cm^2.

2.9. Cell immunostaining for laser scanning confocal microscopy

The behaviour of cells in culture on the different membranes was analysed by Laser Scanning Confocal Microscopy (LSCM, Fluoview FV300, Olympus) after the immunostaining of actin cytoskeleton protein, vinculin focal adhesion protein, markers of mature liver, namely albumin and cytokeratin 18 (CK18), and hepatoblasts alfa feto protein marker (AFP).

Hepatocytes in the membrane systems were fixed in 4 % (*w*/*v*) paraformaldehyde for 15 min, followed by permeabilization and blocking with a solution containing 0.3 % *v*/v Triton X-100 and 10 % v/v foetal bovine serum (FBS, Euroclone, Italy) in PBS for 1 h at 37 °C. Samples were then incubated overnight at 4 °C with the following primary antibodies: anti-vinculin (1:200, Santa Cruz Biotechnology), anti-CK18 (1:200, Santa Cruz Biotechnology), anti-Albumin (1:200, (Bethyl laboratories), anti-AFP (1:200, Santa Cruz Biotechnology). Actin was stained with Alexa 488-conjugated phalloidin (Molecular Probes, Eugene, OR). Secondary antibodies, Cy2™-conjugated Affini Pure donkey anti-rabbit IgG, Cy3™-conjugated Affini Pure donkey anti-mouseIgG and a Cy5™-conjugated Affini Pure donkey anti-goat IgG (1:500, Jackson ImmunoResearch Europe Ltd) were then added for 1 h at room temperature. The nuclei of cells were stained with DAPI (200 ng/mL, Molecular Probes). Finally, samples were rinsed, mounted and observed at LSCM.

Quantitative analysis was performed by calculating the percentage of positive cells for each liver marker proteins (albumin, CK18 and AFP positive nuclei) over the total (DAPI-stained nuclei).

The fluorescence intensity for stained actin and vinculin was calculated on LCSM images of cells at DIV13, in a series of squared areas of 235 × 235 μm of the x–y axis vs the z axis of acquired images, using Fluoview 5.0 software (Olympus Corporation). Each image was composed of 20 slices, having an optical thickness of 0.5 μm. Photomultiplier settings were the same for all acquisitions with each dye. Images were acquired from randomly selected fields.

2.10. Glycogen detection

Cells at the endpoint of the differentiation stage were stained using a Periodic acid-schiff (PAS) kit (Sigma Aldrich, Milan, Italy) for glycogen analysis. Cells were fixed in 4 % formaldehyde, permeabilized with 0.1 % Triton X-100 for 10 min, and then oxidized in 1 % periodic acid for 5 min, rinsed 3 times in deionized water (dH_2O), treated with Schiff's reagent for 15 min, and rinsed in dH_2O for 5–10 min. Samples were counterstained with Mayer's hematoxylin (Sigma Aldrich, Milan, Italy) for 1 min and rinsed in dH_2O and finally, the cells were visualized by light microscopy.

2.11. Albumin synthesis

Liver-specific cellular functions were investigated in terms of the capacity of cells to produce albumin which is integral to hepatocytes function. To this end, the supernatants of cell cultures were collected and stored at −20 °C until analysis. The amount of albumin in the medium was determined by a sandwich enzyme-linked immunosorbent assay (ELISA), as previously reported. 96-well plates were coated with 50 μg/mL rat albumin (Sigma, Milan, Italy) and left overnight at 4 °C. After 4 washes, 100 μL of cell culture supernatant was added to the wells and incubated overnight at 4 °C with 100 μL of anti-rat albumin monoclonal antibody conjugated with horseradish peroxidase (Bethyl Laboratories, Inc., United States). After 4 washes, the substrate buffer containing tetramethylbenzidine and hydrogen peroxide (H_2O_2, Sigma, Milan, Italy) was added for 7 min and the reaction was stopped with 100 μL of 8 N Sulfuric acid (H_2SO_4, Sigma Aldrich, Milan, Italy), followed by absorbance measurements at 450 nm with a Multiskan Ex (Thermo Lab Systems).

2.12. Statistical analysis

Statistical analysis was carried out using one-way ANOVA test followed by Bonferroni *t*-test. A value of $p < 0.05$ was considered statistically significant.

3. Results and discussion

3.1. Jellyfish collagen (jCol) extraction and characterization

Over the past few years, studies involving the extraction of collagen from marine sources for applications in the nutraceutical, cosmeceutical, and pharmaceutical industries have been increasing, also highlighted by the growing number of scientific publications [17]. In particular, jellyfish collagen (jCol) currently represents an excellent

alternative to commercially available mammalian collagens.

In this work, we obtained the native form of jCol from *R. pulmo* from fisheries by-catch through the acid-solubilized collagen extraction, avoiding the pepsin digestion step (Fig. 1A), as described in Section 2.2. The use of discarded by-catch species is in line with the development of a sustainable process, providing a possible reduction of fishing discards, in accordance with the recent European Common Fisheries Policy (CFP).

Fibrillar collagen type I is the most abundant protein in vertebrates. It is a heterotrimer consisting of two α1- and one α2-chains, generally of 129 kD and 139 kD, respectively. The SDS-PAGE analysis of extracted jCol showed the characteristic protein bands, corresponding to the molecular mass reported in previous publications on the molecular weight of *R. pulmo* collagen [16,18] (Fig. 1B). Higher molecular weight bands were also observed indicating the presence of β- (approximately 260 kD) and γ- (>350 kD) chains, suggesting the existence of dimers or trimers of α chains, respectively [19]. Moreover, no differences in the protein patterns between *R. pulmo* umbrella or oral arms were observed. It is important to consider that the triple-helical proteins exhibit an apparent electrophoretic mobility that is not related to their molecular masses, due to the low content of hydrophobic residues. As expected

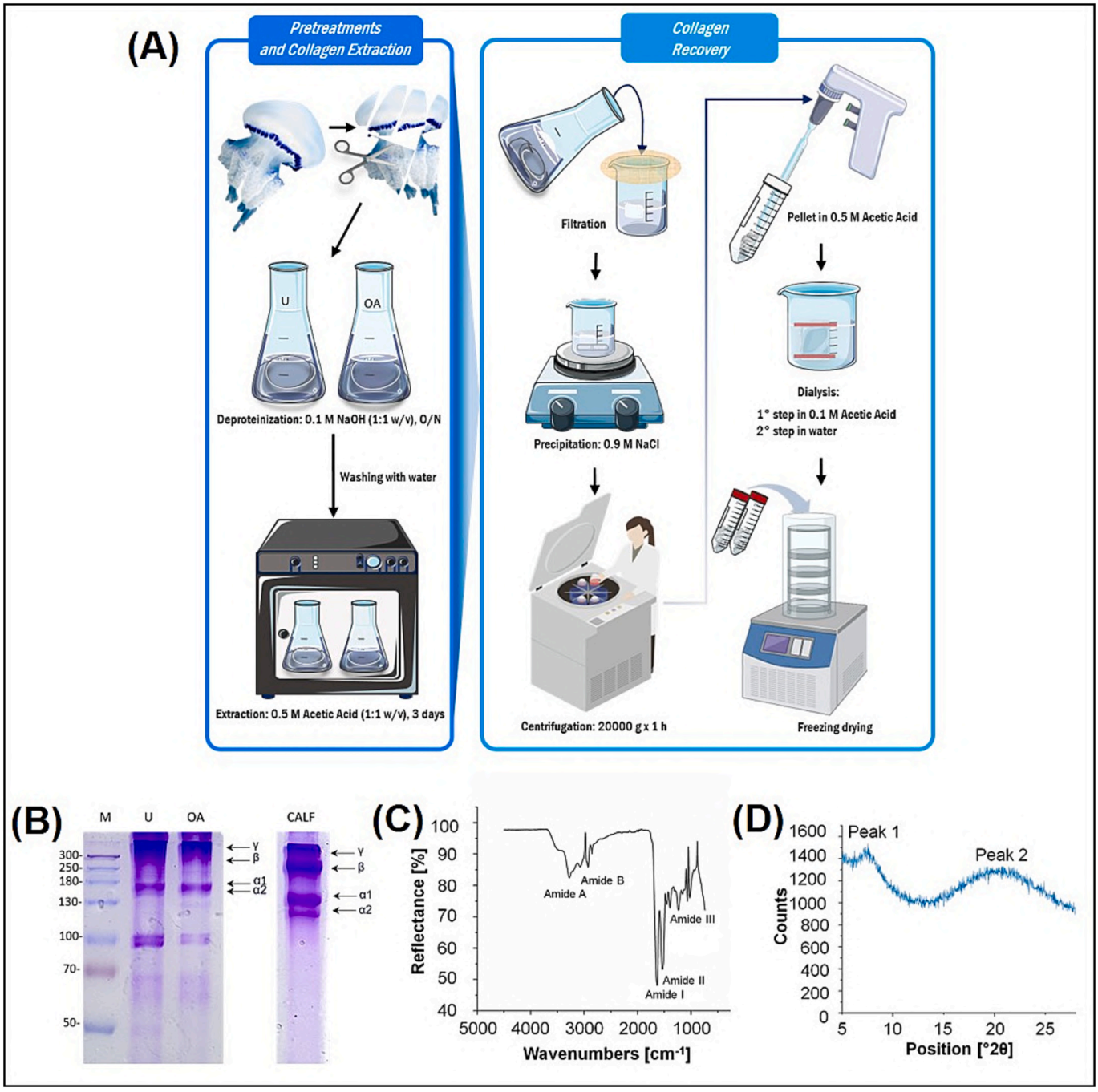

Fig. 1. Jellyfish Collagen (jCol) extraction and characterization.
(A) Representative Scheme of the collagen extraction process from jellyfish.
(B) SDS-PAGE analyses of *R. pulmo* umbrella (U) and oral arms (OA) collagen; Calf type I collagen (CALF); M represents molecular weight markers in kDa.
(C) ATR -FTIR spectrum of jCol between 4500 and 500 cm^{-1}.
(D) X-ray diffraction pattern of jCol.

from the literature, the bands corresponding to the α and β chains of the extracted jCol have a slightly higher apparent molecular mass than the calf counterpart (Fig. 1B). This could be due to the different amino acid composition of *R. pulmo* collagen, containing less hydroxyproline, proline, glycine, and glutamic acid residues than mammalian type I collagen [20]. However, although these residues are involved in the formation and stability of the quaternary structure of type I collagen, they do not appear to influence the structure of collagen [21].

As shown in Fig. 1C, the ATR-FTIR spectrum of the jCol exhibited the representative peaks attributed to amide A, amide B, amide I, amide II, and amide III. For instance, the band position of amide A was found at 3278 cm^{-1} and corresponded to stretching vibrations of N—H, that

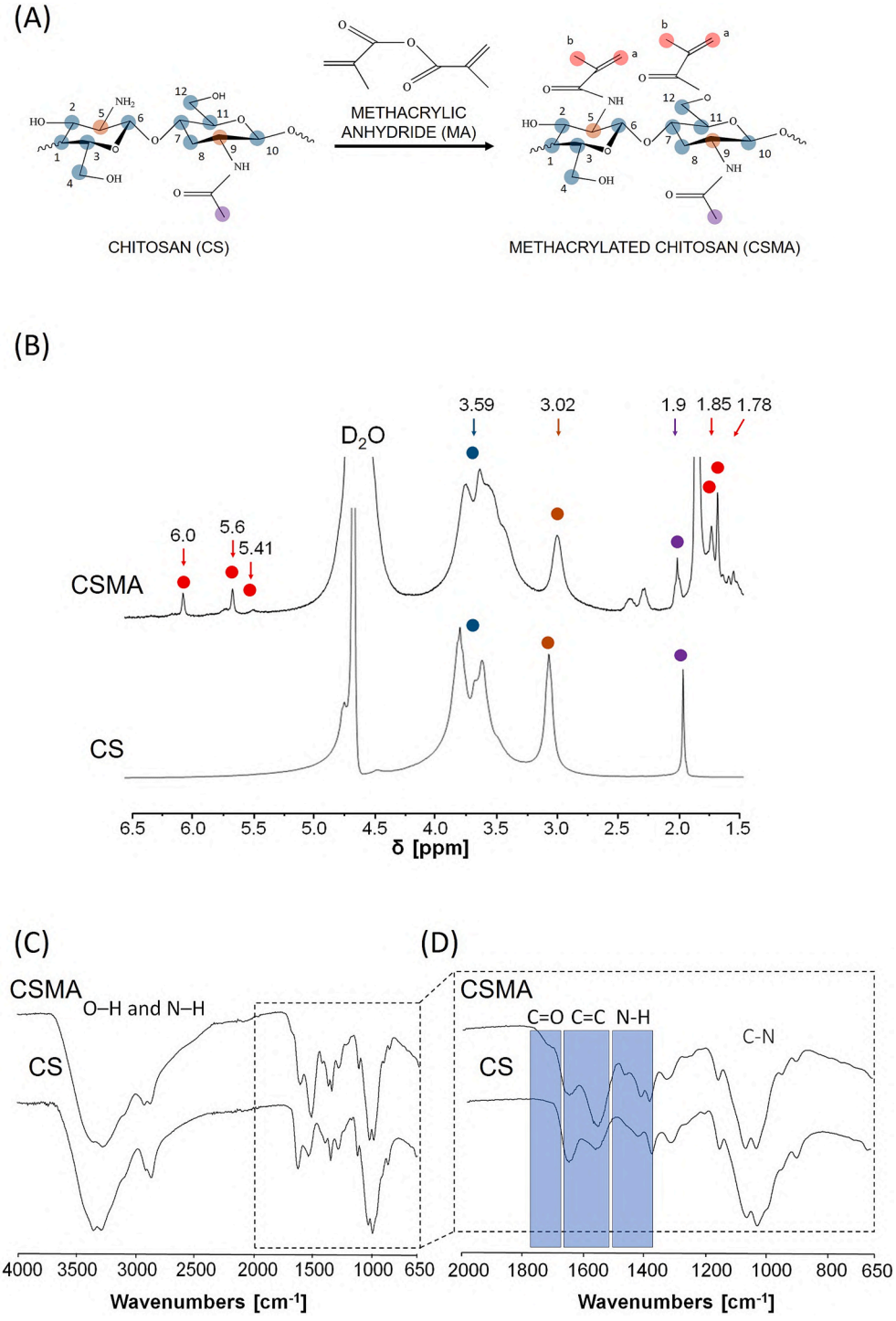

Fig. 2. CSMA synthesis and characterization.
(A) Representative scheme of reaction between Chitosan (CS) and methacrylic anhydride (MA) to obtain methacrylated chitosan (CSMA).
(B) ^{1}H NMR of CS and CSMA.
(C) ATR-FTIR of CS and CSMA between 4000 and 650 cm^{-1}.
(D) ATR-FTIR of CS and CSMA between 2000 and 650 cm^{-1}. Both analyses highlighted the success of the functionalization reaction, reporting the typical functional groups and the moieties introduced by the methacrylation reaction.

generally occur at 3400–3440 cm^{-1} when the N—H group is free from hydrogen bonding [22]. In this work, the band position resulted at low frequency, suggesting that N—H groups were involved in the hydrogen bond formation which helps to hold the triple helical structures together within the collagen molecule [23]. The band position of amide B was observed at 3069 cm^{-1} and correlated to asymmetrical stretching of CH_2 [22]. The peak for amide I is usually observed in the range of 1600–1700 cm^{-1}, which is generated by stretching vibration of C═O in polypeptide backbone of protein. This is the sensitive area of changes of protein secondary structure, and often used for protein secondary structure analysis. The amide I peak of jCol occurred at 1632 cm^{-1}. The presence of amide II was observed from the peak at 1531 cm^{-1} attributed to NH bending vibration coupled with CN stretching. Amide III band was found at wavenumber of 1231 cm^{-1} which corresponds to the stretching vibrations of C—H. Absorption bands around 1390–1455 cm^{-1} were also found. These bands can be ascribed to pyrrolidine ring vibration of hydroxyproline and proline. This result indicated that the triple helical structure of jCol was well preserved during extraction process [24]

The X-ray diffraction pattern of lyophilized jCol is reported in Fig. 1D. There were two diffraction peaks, located at diffraction angles (2θ) of 7.50° and 20.69°, corresponding to the characteristic diffraction peaks of collagen which contains proteins having ordered structure or ordered structure snippet [25]. The first peak, labelled 1, was sharp while the second one, labelled 2 was wide. These peaks correspond to two *d*-spacing at 11.77 (d_1) and 4.28 Å (d_2), which were attributed to the diameter of the triple-helix collagen molecule and the single left-hand helix chain, respectively [26]. The minimum values (d) of the repeat spacing were calculated from the Bragg equation $d(Å) = \lambda/2\sin\theta$ where λ is the X-ray wavelength (1.54 Å) and θ is the Bragg diffraction angle [26]. The obtained results were in accordance with the diameter of a standard collagen molecule with a triple-helix with a single left-handed helix chain. Therefore, it is possible conclude that the collagen after the extraction process was still in its natural conformation and not denatured.

3.2. CSMA synthesis and characterization

In this study, CS was methacrylated by reaction with MA, as schematically reported in Fig. 2A. This strategy has the benefit of allowing chemical crosslinking thanks to the methacrylate group's C═C bond. The success of the methacrylation reaction was confirmed by ^1H NMR and ATR-FTIR (Fig. 2B, C and D). The CS spectrum displays the typical CS peaks: the quadruplet peak at $\delta = 3.59$ ppm related to the protons in 1–4, 6–10, 12 positions and the peak at 3.02 ppm ascribed to the protons in 5, 11 positions of the CS ring (Fig. 2B). The peak at $\delta = 1.9$ ppm represents the (*N*-acetyl)-D-glucosamine group. In the CSMA spectrum, new peaks can be observed at $\delta = 6.0$, 5.60 and 5.41 ppm, representing the $= CH_2$ of the methacrylic double bonds, and at $\delta = 1.85$ and 1.78 ppm corresponding to the $-CH_3$ methyl groups of the grafted methacrylated moieties. There are two types of $-CH_3$ signals and three different peaks corresponding to the $= CH_2$ protons, meaning that the methacrylated groups are successfully grafted to both the $-NH_2$ and the −OH groups of the CS [8,27] (Fig. 2B).

ATR-FTIR spectra of CS and CSMA are reported in Fig. 2C and D. Similar regions of both spectra were observed, such as the characteristic broad peak from 3000 cm^{-1} to 3600 cm^{-1}, which indicates the presence of hydroxyl, amino and hydrogen-bonded (−OH) groups, and absorption bands for CS at 1026–1151 cm^{-1} (amine C—N stretch) (Fig. 2C). In both spectra, the peak between 2850 and 2950 cm^{-1} can be ascribed to the CH stretching of the alkyl groups. However, the increase in the intensity of the absorption bands is well evident in CSMA spectrum (Fig. 2C). Particularly, in this spectrum, the presence of a new peak at 1720 cm^{-1}, ascribable to the amide C═O stretching vibrations, can be noticed, and it confirms the methacrylation of CS. Furthermore, the appearance of a double bond signal at 1537–1653 cm^{-1} depicted alkenyl C═C stretch. However, significant changes were observed in the absorption peaks at 1550 cm^{-1} and 1640 cm^{-1}, associated to the amine vibration and methacrylate C═C, respectively, partially overlapping the amide I peak (~1650 cm^{-1}) [8,27] (Fig. 2D).

3.3. Characterization of membranes

In the present study, new biomimetic composite membranes were developed by blending modified CSMA with jCol.

CSMA membrane and CSMA/jCol blended membranes were prepared in flat configuration using the phase inversion technique inducing precipitation by solvent evaporation. For the composite membranes, the jCol solution was added to the CSMA solution by combining the components in two different ratios, 70 % chitosan/30 % collagen, and 50 % chitosan/50 % collagen, generating two different membranes namely CSMA/jCol30 and CSMA/jCol50, respectively. The properties of the developed membranes, including chemical composition, surface morphology, roughness parameters, mean pore size, wettability, mechanical qualities, degradability, and cell growth were all deeply analysed considering their pivotal role for tissue engineering applications, and summarized in Table 1.

Surface topography is an important factor that influences cell adhesion and growth affecting cell-membrane interactions [28]; thus, the surface morphology and roughness of each membrane were also investigated (Fig. 3). SEM observation revealed that CSMA and CSMA/jCol membranes had a homogenous and compact surface looking quite similar (Fig. 3A-C). The smooth surface of the blended membranes suggested that a homogenous blending of the two biopolymers properly occurred in both composite membranes. The successful blending is related to the formation of hydrogen bonding between the NH_2 and OH groups in the functionalised CS and jCol. This result is in line with other studies, in which SEM analysis displayed a very smooth surface of CS/collagen biomaterials [29].

Consistently with SEM results, the AFM analysis highlighted the uniform smooth surface of all the investigated membranes and confirmed the successful combination of marine collagen and functionalized CS (Fig. 3D-F). CSMA membranes exhibited roughness values of 2.9 ± 0.3 nm and 3.7 ± 0.3 nm of Ra and Rq, respectively. Meanwhile, CSMA/jCol membranes highlighted higher values of Ra and Rq, reaching 3.6 ± 0.4 (Ra) and 4.7 ± 0.9 nm (Rq) for CSMA/jCol30 membranes and 3.9 ± 0.4 and 4.7 ± 0.9 nm for CSMA/jCol50, as reported in the Table 1.

Porometer measurements revealed nanopores with diameters of about 26.5 ± 7.0, 47.2 ± 4.2 and 49.7 ± 8.3 nm for CSMA, CSMA/jCol30, and CSMA/jCol50 membranes, respectively. These results suggest that the addition of marine collagen significantly increased the pore size diameter of the pure CSMA membrane, in agreement with other studies [29,30]. Moreover, the increased roughness of CSM/jCol membranes could be ascribable to the presence of increased nanopores on their surface compared to CSMA ones.

ATR-FTIR spectra reported in Fig. 4 A enable to identify the

Table 1
Membrane properties. Thickness; mean pore diameter; Average roughness (R_a) and the root mean squared roughness (R_q); Water Contact Angle (WCA); Young's modulus (E); Elongation at break (ε); Ultimate tensile strength (UTS). Results are expressed as mean value ± standard deviation (SD).

	CSMA	CSMA/jCol30	CSMA/jCol50
Thickness [μm]	27.2 ± 8.0	22.1 ± 4.0	21.7 ± 6.0
Mean Pore Diameter [nm]	26.5 ± 7.0	47.2 ± 4.2	49.7 ± 8.3
Roughness [nm]	Ra: 2.9 ± 0.3 Rq: 3.7 ± 0.3	Ra: 3.6 ± 0.4 Rq: 4.7 ± 0.9	Ra: 3.9 ± 0.3 Rq: 4.9 ± 0.4
WCA [°]	84.4 ± 3.4	76.6 ± 2.6	71.2 ± 6.0
E [MPa]	611.0 ± 81.0	418.0 ± 82.0	364.0 ± 34.0
ε [%]	1.6 ± 0.2	3.0 ± 0.9	4.4 ± 0.9
UTS [MPa]	51.7 ± 6.0	29.9 ± 8.6	22 ± 3.0

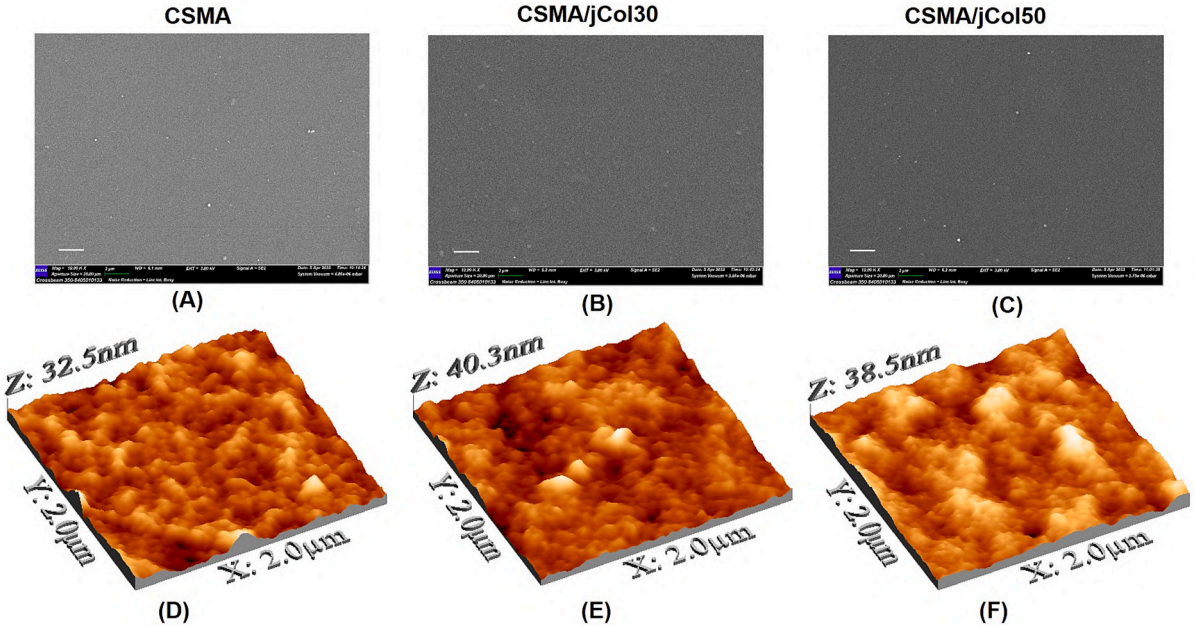

Fig. 3. Membrane surface morphology.
Scanning electron micrographs (A-C) and AFM images (D-F) of the surface of CSMA (A and D), CSMA/jCol30 (B and E) and CSMA/jCol50 (C and F) membranes. Scale bar of SEM micrographs: 2 μm.

vibrational bands corresponding to both polymers' primary functional groups. The spectra related to CSMA/jCol membranes show the characteristic bands of chitosan, with the broad band in the region of 3700–3100 cm^{-1}, ascribed to the axial deformations of the O—H and N—H groups and the region between 2800 and 3000 cm^{-1} from -CH_2 and -CH_3 ones, presented in the polysaccharide structure, as also reported in Fig. 2 C and D. Furthermore, the spectra also show the characteristic peaks at 1640 and 1550 cm^{-1} of C═O and N—H stretching, ascribable to protein amide I and amide II of collagen, as recognized in Fig. 1 C. Even though it is particularly difficult to analyse the peaks due to the partial overlapping, some differences of the intensity of their characteristic peaks were observed between the two compositions, mainly related to the different concentration of both polymers. Particularly, the intensity of those peaks seems slightly higher in CSMA/jCol50 membrane where there was a higher collagen concentration [31].

An important characteristic of these membranes is the transparency that allows a microscopic observation of the cell culture during the experimentation.

Since surface topography influences the physicochemical properties that in turn would affect cell adhesion, we investigated the wettability of the membranes by WCA measurements (Table 1). CSMA membrane displayed values of 84.4 ± 3.4° that indicate a slight hydrophobic character due to the functionalization with MA. The blend with jCol at different concentrations gave arise to a more hydrophilic material. It caused a significant decrease to value of 76.6 ± 2.6° in CSMA/jCol 30 membranes. A further reduction of the WCA occurred by increasing the collagen concentration to 50 % (CSMA/jCol50) and, indeed, this membrane showed a moderate hydrophilic character with a contact angle of 71.2 ± 6°. These findings clearly indicate that marine collagen blending successfully balanced the hydrophobic character of CSMA membranes, leading to the formation of new materials with moderate wettability able to promote cell attachment and growth. As a structural protein, collagen contains many hydrophilic groups (i.e. NH and OH groups), and when it is added to a hydrophobic polymer, like CSMA of our study, the WCA of the pure CS membranes was significantly decreased, obtaining a new material with improved wettability, in good agreement with other papers [29,32].

Due to the need of providing a certain structural stability during culturing *in vitro* and implanting *in vivo*, the mechanical properties play a pivotal role in the engineering of suitable membranes that can significantly affect the specific biological functions of cells. In general, the mechanical strength mainly depends on structural parameters such as pore size and porosity, but it can be strongly affected by the material components and crosslinking. CS is a biomaterial widely used in a variety of biomedical applications, nevertheless, non-crosslinked CS has very poor mechanical features. In our paper, to make CS strong enough to be used in the bioartificial liver, it was functionalized with MA to be photocrosslinked using Irgacure as an initiator under UV light. Young's modulus (E), ultimate tensile strength (UTS) and elongation at break (ε) were assessed via uniaxial tension. These parameters indicate the stiffness, strength, and elasticity of the membrane, and are important mechanical features in supporting the tissue engineering application of the membrane (Table 1). CSMA membrane developed in this study displayed a value of E of 611.0 ± 81.0 MPa, thanks to the MA functionalization. Moreover, marine collagen incorporation induced a decrease in stiffness of the native CSMA membranes, which allowed obtaining membranes with suitable mechanical properties for the specific application [29,33]. Indeed, E values of CSMA/jCol membrane decreased to 418.0 ± 82.0 MPa and 364.0 ± 34.0 for CSMA/jCol30 and CSMA/jCol50 membranes, respectively. Regarding UTS, the same decreasing trend was observed: for CSMA/jCol30 membrane was detected a value of 29.9 ± 8.6 and for the CSMA/jCol50 one, a value of 22 ± 3 MPa, which are significantly lower than that of the native CSMA membrane (51.7 ± 6 MPa). Membranes have different percentage of elongation at break, which was found in the following order CSMA/jCol50 (4.4 ± 0.9 %) > CSMA/jCol30 (3 ± 0.9 %) > CSMA (1.6 ± 0.8 %). Therefore, the marine collagen blend resulted in an enhancement of the elastic properties as demonstrated by the significant decrease of Young's modulus and the tensile strength, and the increase of the elongation at break, in accordance with the literature [29,33]. The improving value was probably related to the formation of an attractive interaction between the functionalized chitosan and marine collagen in the blended membranes since the successful integration of two polymer components depends on the intermolecular interactions, which results in an improved quality of the blend mechanical properties.

Another pivotal factor required for an ideal material for tissue

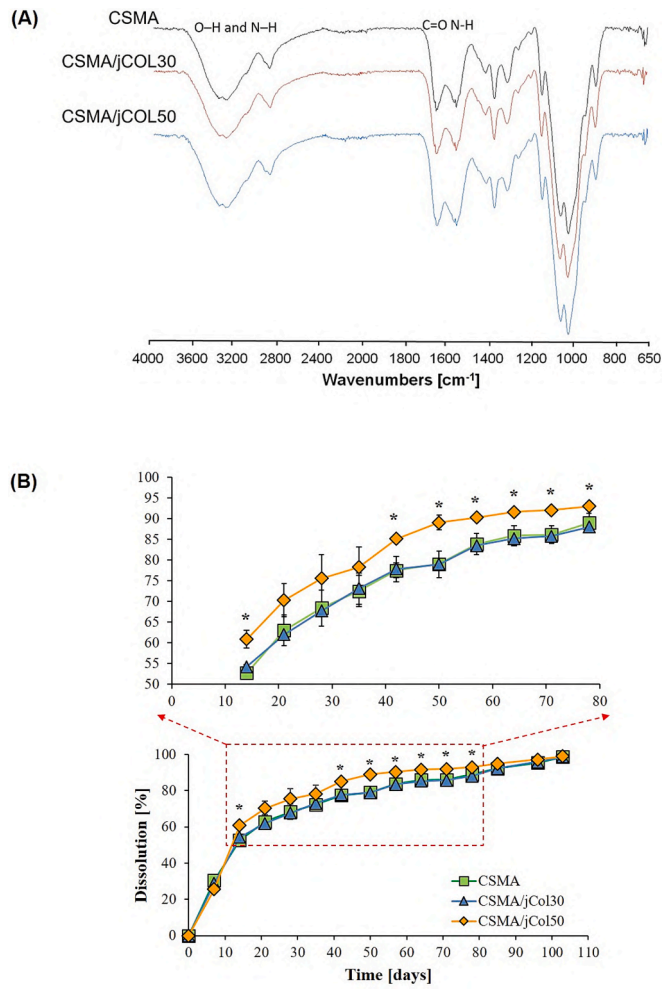

Fig. 4. Chemical composition and degradability of membranes.
(A) ATR-FTIR of CSMA and CSMA/jCol membranes between 4000 and 650 cm^{-1}.
(B) Dissolution behaviour of (□) CSMA, (Δ) CSMA/jCol30 and (◆) CSMA/jCol50 membranes as a function of time. The values expressed as average ± SD are the means of 10 measurements per sample, and data statistically significant were evaluated according to ANOVA followed Bonferroni *t*-test ($p < 0.05$): * vs CSMA and CSMA/jCol30 membranes at the same day.

engineering is an appropriate degradation capacity. Materials should provide sufficient mechanical stability during the time needed for tissue repair and then progressively degrade allowing the new tissue formation. Fig. 4B shows the degradation of membranes in a PBS solution containing lysozyme. Usually, pure CS membranes entirely degrade after few days, while our results highlighted that the modification with MA slowed down the CS degradability by modulating and preserving membrane structural and mechanical integrity for a longer period of time (103 days). Dissolution of all membranes increased with time: over the first 14 days, it was very fast reaching value of 61 ± 2 %, for CSMA/jCol50 membrane, 54 ± 1 % for CSMA/jCol30 membrane and 52 ± 1 % for pure CSMA. Afterwards, membrane dissolution was slower and stable within time, especially from day 42 to day 103, when all membranes were completely dissolved. Interestingly, from day 42 to day 78, CSMA/jCol50 membrane displayed higher values of dissolution ($p < 0.05$) than CSMA and CSMA/jCol30 membranes, probably due to its higher collagen content that contributes to a faster degradation. Thereafter, no differences were observed among the membranes that exhibit the same dissolution percentage, probably related to the CSMA content.

Membrane characterization data highlighted that the addition of marine collagen to CSMA enhanced important properties such as pore size, physicochemical and mechanical characteristics leading to the development of advanced biomimetic membranes that have potential to be used in tissue engineering applications.

3.4. Membrane properties influence liver cell behaviour

Membrane systems are able to promote cell proliferation and differentiation towards the formation of liver tissue [4–6]. They can act as a synthetic ECM thanks to polymer properties (e.g., biocompatibility, biofunctionality) and distinctive intrinsic membrane characteristics such as permeability, selectivity, stability, and a well-defined geometry [5].

In our study, the potential of the membranes produced with CSMA and marine collagen as new generation of sustainable biomimetic materials for liver tissue engineering was addressed by culturing rat embryonic liver cells. Previous papers employed these cells as an alternative model of human liver progenitor cells, since using cells from the foetal human liver is limited by major ethical issues. In those works, the membranes were able to promote the expansion and functional differentiation of rat embryonic liver cells in comparison with traditional substrates [34,35].

Our aim was to validate the suitability of the new marine collagen-blend membranes to support liver tissue engineering with special attention to the influence of membrane properties on liver cells behaviour. Therefore, the ability of the developed membranes to offer to the cells a specific and familiar *milieu* for the embryonic liver cells commitment was deeply investigated.

The biocompatibility was investigated by culturing embryonic liver cells in direct contact with the different membranes. Then, cell viability, morphology and cytoskeleton organization were analysed (Fig. 5). We evaluated the role of membrane properties and collagen content in determining their efficiency for liver tissue regeneration.

SEM analysis, after 14 days of culture, showed that the cellular reorganization over the three substrates was quite similar (Fig. 5A). On membranes, cells adhered, spread, and acquired a polyhedral shape morphology, which is typical of differentiated and mature hepatocytes. Very tight cell-cell interactions with the formation of multilayers were also visible on all membranes. However, morphological cell features changed by modulating the membrane composition and properties. When cells were cultured on CSMA membrane, the most hydrophobic and stiff material, they displayed a very flat and spread morphology, with a nonuniform distribution and empty spaces over the surface (Fig. 5A, Panel I). In the case of composite membranes, the blending with jCol significantly improved mechanical stability, enhancing also hydrophilic properties, thus favouring the interactions with cells. Coherently, as highlighted by Fig. 5A, on CSMA/jCol30 (Panel IV) and CSMA/jCol50 (Panel VI) membranes, cells formed intercellular tight contacts and even the degree of a multi-layered cell aggregation is visibly higher than on CSMA membranes (Panel II), achieving the formation of a complex 3D construct. This is an important result, because it is well known that the cell-cell and cell-material interactions are crucial for the maintenance of hepatocyte phenotype and specific functions. Moreover, blended membranes appeared completely covered by multilayers of cells that assembled themselves in 3D cord-like structures acquiring a tissue-like phenotype with features like that of liver parenchyma [34,35].

To further characterize the liver cell behaviour on these membranes, immunocytochemistry investigation was carried out by LSCM. Consistent with SEM analysis, confocal images (Fig. 5B) indicated that membranes supported adhesion and growth of liver cells. Staining for the cytoskeletal protein actin (in green) and the focal adhesion marker, vinculin (in red), demonstrated the overall morphology of the cells cultured and the organization of the cytoskeletal proteins on CSMA and CSMA/jCol membranes. Cells grown on CSMA (Fig. 5B, Panel I), CSMA/jCol30 (Fig. 5B, Panel II) and CSMA/jCol50 membranes (Fig. 5B, Panel III), appeared well spread and acquired a polyhedral shape morphology

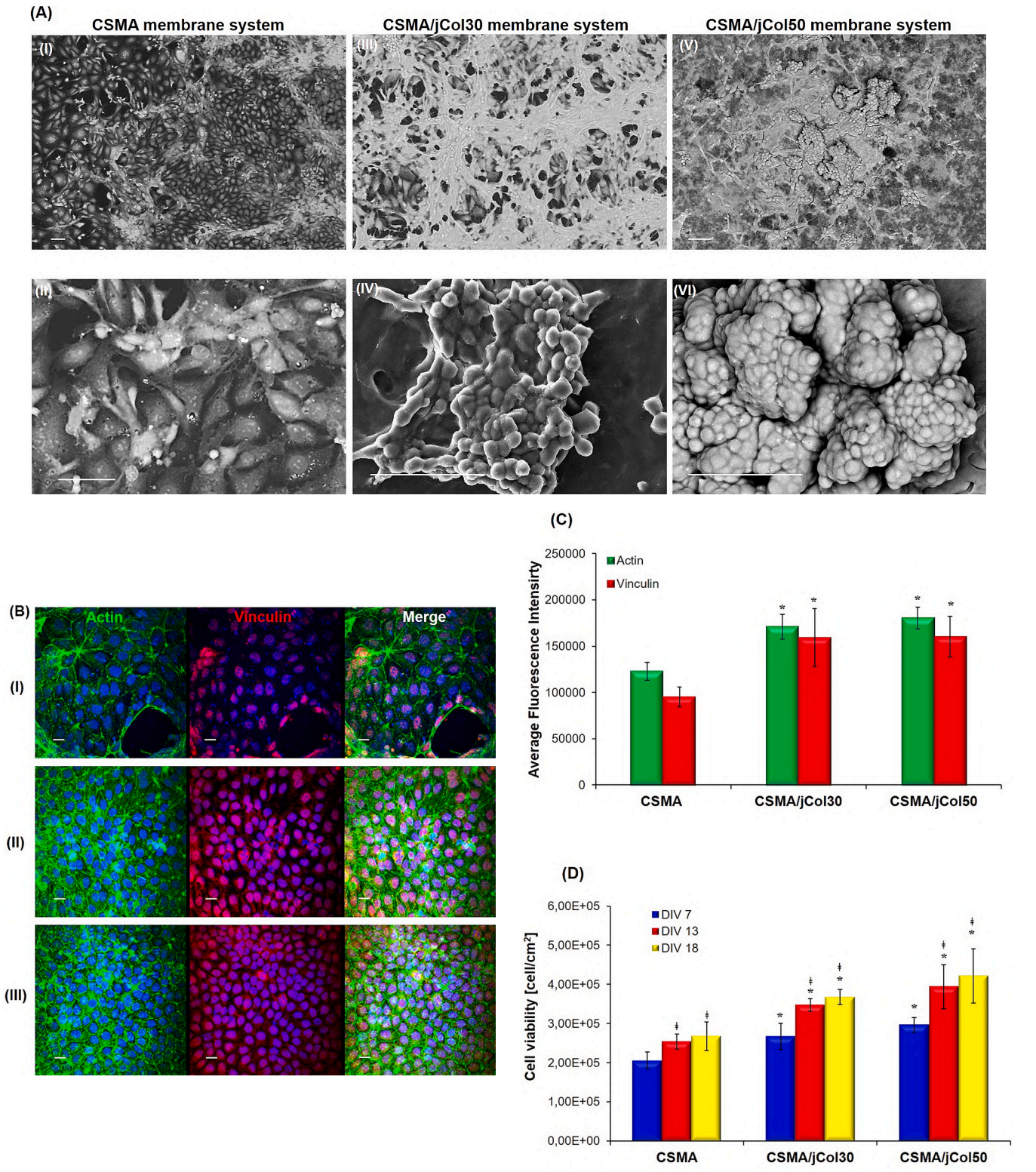

Fig. 5. Behaviour of embryonic liver cells in the different membrane systems.
(A) SEM images at different magnifications of liver cells at DIV14 on: (I-II) CSMA, (III-IV) CSMA/jCol30, (V-VI) CSMA/jCol50 membranes. Scale bar: 50 μm.
(B) Confocal laser micrographs of liver cells after 14 days of culture in the different membrane systems (I) CSMA, (II) CSMA/jCol30, (III) CSMA/jCol50 membranes. Cells were stained for actin (green), vinculin (red) and nuclei (blue). Scale bar: 20 μm.
(C) Average fluorescence intensity for stained actin (green bar) and vinculin (red bar) of cells at DIV13 on the different membranes. Data statistically significant according to ANOVA followed Bonferroni t-test; *$p < 0.05$ vs CSMA membrane.
(D) Changes in cell viability of liver cells after 7, 13 and 18 days of culture in the different membrane systems. The values expressed as average ± SD are the means of 5 experiments and data statistically significant were evaluated according to ANOVA followed Bonferroni t-test ($p < 0.05$): * vs CSMA membrane at the same DIV; ‡ vs the same membrane at DIV7.

as hallmark of differentiated liver cells. On all kinds of membranes, the expression and pattern distribution profile of actin and vinculin showed up a cell displacement according to a parenchymal-like structure (Fig. 5B). A dot-like distribution of vinculin also highlighted the numerous cell−cell and cell−membrane interactions. In order to evaluate the changes in the expressions of cytoskeletal and focal adhesion markers, quantitative analysis in terms of the fluorescence intensity of actin and vinculin was then performed (Fig. 5C). The fluorescence intensity of both investigated markers was significantly higher in cells cultured on blended membranes with respect to CSMA membranes. The permissive surrounding within these membrane systems favoured specific liver features development, recapitulating those of the natural liver.

These results were confirmed by cell viability data. As shown in Fig. 5D, the number of viable cells on each membrane significantly increased ($p < 0.05$) after 18 days in vitro, suggesting that these biomaterials have appropriate features in terms of biocompatibility and nontoxic response that validate their use for the realization of promising tissue engineered liver constructs. Our investigation showed a distinct biocompatibility degree for the different membranes. The highest cell viability was assessed on membranes with the highest collagen content (CSMA/jCol50 membranes). Cell number on these membranes was similar to the ones on CSMA/jCol30 membranes by day 7; cell expansion within time was quite comparable on these two surfaces. Interestingly, at each culture time point, cell viability on both marine collagen-blended membranes was significantly higher than on CSMA membrane. It was noticed that after 18 days of culture on CSMA/jCol30 ($3.7 \pm 0.2 \times 10^5$ cell/cm^2) and CSMA/jCol50 ($4.2 \pm 0.7 \times 10^5$ cell/cm^2) membranes, the cells showed 37 % and 57 % higher viability than on the pure CSMA membrane ($2.7 \pm 0.4 \times 10^5$ cell/cm^2), respectively. This agrees with SEM and LSCM analysis: the cells on blended membranes were very close to each other then, they communicated more easily and could proliferate to a much higher number of cells compared to CSMA membrane where cells did not completely cover their surface. These results are strictly related to the high biocompatibility of collagen and to its good and uniform dispersion in the CSMA solution, which improved hydrophilicity and mechanical stability of the blended membranes. It is reported that the adhesion of hepatocytes to collagen substrate regulates functional behaviour. Furthermore, adhesion, morphological features, and viability of cells are strongly affected by the properties of the membrane on which they are seeded, as suggested by previous works, showing a relationship between cell adhesion and membrane surface hydrophilicity [29]. In this scenario, our CS-based membranes offered the cells a matrix that is similar to glycosaminoglycans of the liver ECM and favoured the initial step of cell adhesion due to interaction of its protonated NH_2 groups with anionic functional groups on the cellular membrane. However, despite the promising effect of collagen and CS-based materials in hepatocyte cultures, only a few studies described the impact of CS/collagen composites for liver tissue engineering [7,36–37] and even less work is focused on marine collagen [32,38]. For this reason, the present work is pioneering investigation that reports the combination of marine collagen with CSMA as support for the culture of liver cells.

3.5. Membranes boost hepatocyte differentiation and specific liver tissue functions

The capability of the different membrane systems to boost liver differentiation was further investigated by observing the expression profile of distinctive hepatic lineage markers. LSCM analysis was carried out after immunostaining of albumin, a typical marker of mature hepatocytes, cytokeratin 18 (CK18), a marker expressed by several liver cell types, including bile ductal epithelial cells and hepatocytes, and alfa-fetoprotein (AFP), a serum glycoprotein produced by liver during fetal life, a typical marker of hepatoblasts and foetal hepatocytes.

The initial cell suspension before seeding was AFP-positive with a very low expression of albumin (data not shown), as reported in a previous paper [35]. In our study, after 14 days of culture on the developed membranes, cells displayed low AFP expression, while albumin and CK18 were highly expressed and widely distributed, mainly localized on the cell membrane, which is consistent with their native distribution in liver [39]. In line with other studies [35–36,40], cells cultured onto the membranes lost their progenitor characteristics related to the AFP expression and gained more differentiated features, as a result of the high expression of albumin and CK18, markers of mature liver cells. These findings suggest that all membranes promoted cell differentiation towards a liver phenotype.

In addition, to investigate cell functionality within the different membrane systems, we tested the ability of the differentiating cell populations to store glycogen, a characteristic of functional hepatocytes. Cells at DIV 14 were stained for cytoplasmic glycogen using the PAS staining procedure (Fig. 6A). Cytoplasm of majority of the cells was stained pink to dark red-purple, indicating the capacity to store glycogen like functional hepatocytes. Hence, consistent with the acquisition of expression of mature hepatic markers, the differentiating cells cultured on all the developed membranes, also exhibited a progressive gain of hepatic functionality in terms of glycogen storage.

To ascertain any differences among the developed membranes in dictating the hepatic differentiation, a quantitative analysis of liver functional phenotype was performed (Fig. 6B). The profile expression patterns for each of the above-mentioned liver markers was quantified and expressed as the percentage of positive cells over the total number of cells within the investigated image field (Fig. 6B). The analysis revealed that, after 14 days, the percentage of albumin-positive cells on CSMA/jCol30 and CSMA/jCol50 was 93.0 ± 3.0 % and 96.0 ± 2.0 %, respectively, which are values significantly higher compared with the CSMA membranes (71.0 % ± 4.0 %). The number of cells expressing CK18 was significantly higher than the one calculated for other membranes with a percentage in the following order: CSMA/jCol50 (79.0 ± 9.0 %) > CSMA/jCol30 (64.0 ± 7.0 %) > CSMA (41.0 ± 1.0 %). Interestingly, the values referred to the membrane with the highest collagen content resulted 2-fold higher than the pure CSMA membrane. Although the percentage of AFP-positive cells on CSMA membrane was kept at low level (17.0 ± 1.0 %), it was significantly higher than on collagen-blended membranes and the values followed the order CSMA > CSMA/jCol50 (9.0 ± 1.0 %) > CSMA/jCol30 (7.0 ± 3.0 %). This may indicate that the state of some cells on CSMA membrane was still at an early stage of differentiation.

Since albumin is a specific and the most abundant protein that can only be synthesized by functioning mature hepatocytes, we examined the cells grown onto the different membranes for albumin secretion, to determine whether the hepatocytes were functionally active. We found that the albumin synthesis rate was maintained throughout the 18-day experiment period and increased continuously over time in all membrane systems, as shown in Fig. 6C. Therefore, the data highlight that all investigated membranes are able to trigger specific metabolic liver functions. During the first 8 days albumin secretion was stable at values of 374.0 ± 8.0 pg/h on CSMA, 458.0 ± 22.0 pg/h on CSMA/jCol30 and 499.0 ± 69.0 pg/h on CSMA/jCol50 membrane, respectively. Then, for each membrane, it rapidly increased reaching its peak values at day 13 and remaining at these levels up to the end of culture. Indeed, at this time frame, the level of albumin synthesis by cells on CSMA membrane (928.0 ± 90.0 pg/h) and collagen blended membrane (1190.0 ± 30.0 pg/h on CSMA/jCol30 and 1203.0 ± 38.0 pg/h on CSMA/jCol50 membrane) was 2-fold and 3-fold higher than those at day 8, respectively. A slight further increase was observed during the last days of culture. Collagen blended membranes enabled albumin synthesis at a greater extent with respect CSMA membrane showing the prominent impact of collagen on albumin secretion, in agreement with previous results [7]. In fact, our data evidence that, for each day of culture, cells on the membrane with the highest collagen content, had the highest metabolic activity. The values of albumin synthesis are significantly higher on blended collagen membranes than those observed when cells

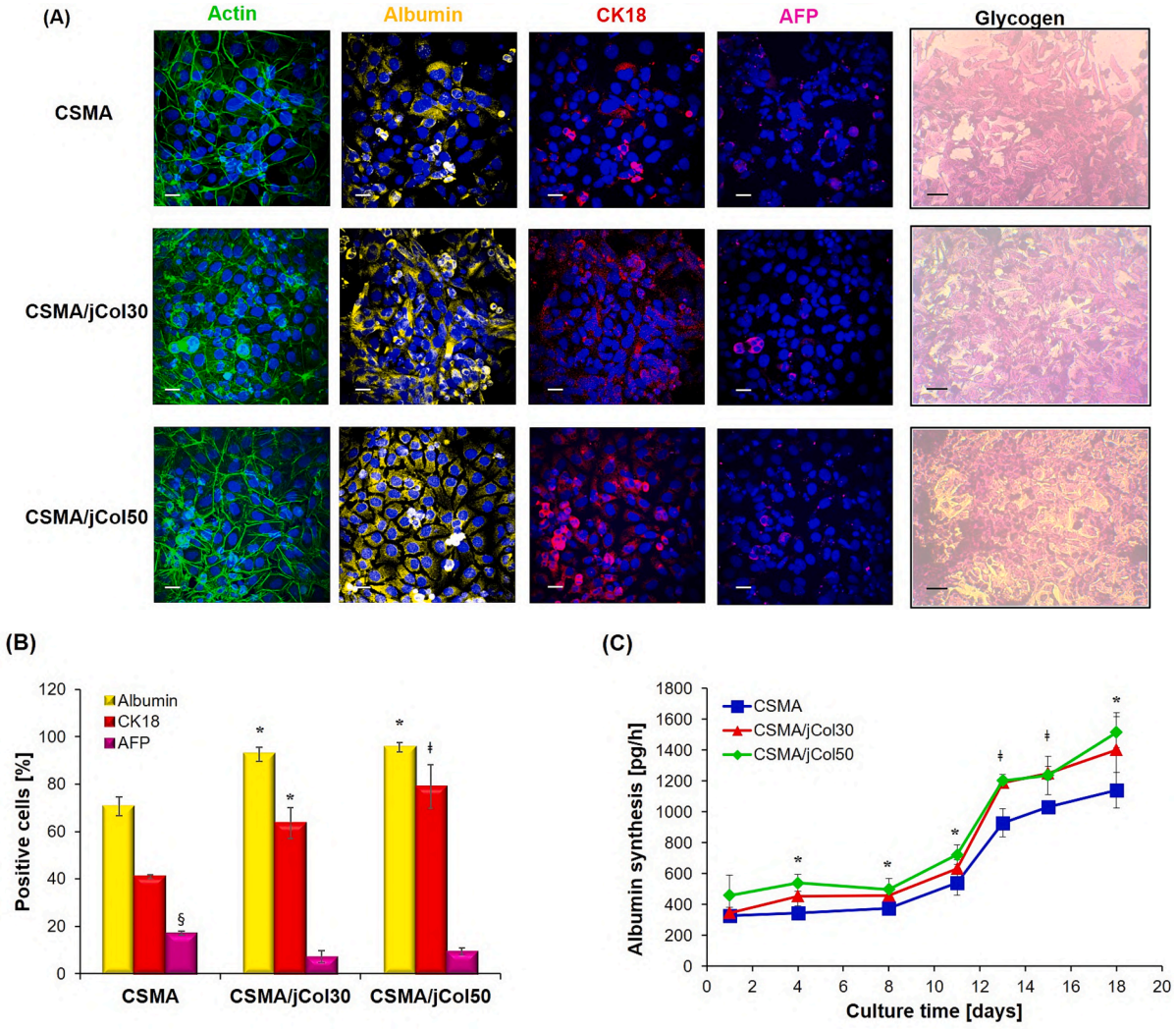

Fig. 6. Liver specific-functions in the different membrane systems.
(A) Confocal laser micrographs of liver cells after 14 days of culture in the different membrane systems. Distribution pattern profile of actin (green), and hepatocytes markers albumin (yellow), CK18 (red) and AFP (magenta). Nuclei are counterstained with DAPI (blue). Scale bar: 20 μm. Light microscope images of Periodic acid–Schiff (PAS) staining of hepatocytes used to detect glycogen storage, scale bar 50 μm.
(B) Quantitative analysis of positive cells for each liver-specific marker. Results are expressed as percentage of positive cells over total and are reported as average ± SD of the means of 5 experiments. Data statistically significant were evaluated according to ANOVA followed Bonferroni t-test ($p < 0.05$): * vs CSMA membrane; ǂ vs CSMA and CSMA/jCol30 membranes; § vs CSMA/jCol30 and CSMA/jCol50 membranes.
(C) Albumin synthesis of liver cells cultured in the different membrane systems. The values expressed as average ± SD are the means of 5 experiments and data statistically significant were evaluated according to ANOVA followed Bonferroni t-test ($p < 0.05$): Within the sane membrane system, albumin synthesis at DIV 13, 15 and 18 is significative vs DIV 1, 4, 8 and 11. *CSMA/jCol50 vs CSMA membrane system at the same DIV; ǂ CSMA/jCol50 and CSMA/jCol30 vs CSMA membrane system at the same DIV.

were cultured on CSMA membranes, consistently with the results of albumin immulocalization data.

4. Conclusions

In this work, we developed sustainable biomimetic membranes by blending of CSMA with jCol and evaluated their properties and biocompatibility for liver tissue engineering applications.

The overall dataset corroborates the complete achievement of differentiation pattern of liver cells cultured on the developed membranes, especially on CSMA/jCol blended membranes. Our approach, based on the combination of functionalized chitosan with marine collagen, significantly improved hepatic differentiation and generated a more reliable *in vitro* tool resembling liver for tissue engineering applications. Furthermore, although many researchers have tried to maintain hepatocyte functions with different culture conditions, our study is the first to show that CSMA/jCol membranes provide a valuable *in vitro* microenvironment, which is able to promote hepatocyte differentiation.

The present work also contributed to highlight the relevance of marine discards for the development of high value-added products, and particularly the use of marine collagen as a good alternative to currently used commercial materials of mammalian origin. In the future, these most promising membranes should be tested *in vivo* to better understand their suitability for the regeneration of liver tissue. These engineered constructs have the potential to address the complex challenges of liver diseases and transplantation, significantly reducing the demand for donor organs, which are often in short supply, and mitigating the risks associated with transplantation.

CRediT authorship contribution statement

Sabrina Morelli: Writing – review & editing, Writing – original draft, Supervision, Methodology, Investigation, Formal analysis, Data curation, Conceptualization. **Ugo D'Amora:** Writing – review & editing, Writing – original draft, Methodology, Investigation, Formal analysis, Data curation, Conceptualization. **Antonella Piscioneri:** Writing – review & editing, Writing – original draft, Methodology, Investigation, Formal analysis, Data curation. **Maria Oliviero:** Writing – review & editing, Writing – original draft, Methodology, Formal analysis, Data curation, Conceptualization. **Stefania Scialla:** Writing – review & editing, Writing – original draft, Methodology, Formal analysis, Data curation. **Alessandro Coppola:** Writing – review & editing, Writing – original draft, Methodology. **Donatella De Pascale:** Writing – review & editing, Writing – original draft, Funding acquisition. **Fabio Crocetta:** Writing – review & editing, Writing – original draft, Methodology. **Maria Penelope De Santo:** Writing – review & editing, Methodology, Formal analysis. **Mariano Davoli:** Methodology. **Daniela Coppola:** Writing – review & editing, Writing – original draft, Methodology, Investigation, Formal analysis, Data curation, Conceptualization. **Loredana De Bartolo:** Writing – review & editing, Supervision, Funding acquisition, Conceptualization.

Declaration of competing interest

The authors declare that they have no known competing financial interests or personal relationships that could have appeared to influence the work reported in this paper.

Data availability

The data presented in this study are available on request from the corresponding author.

Acknowledgement

This work was supported by EU funding within the NextGeneration EU-MUR PNRR Extended Partnership initiative on Emerging Infectious Diseases (Project no. PE00000007, INF-ACT) and by NBFC, funded by the Italian Ministry of University and Research, PNRR, Missione 4 Componente 2, "Dalla ricerca all'impresa", Investimento 1.4, Project CN00000033.

References

[1] S. Morelli, A. Piscioneri, G. Guarnieri, A. Morelli, E. Drioli, L. De Bartolo, Anti-neuroinflammatory effect of daidzein in human hypothalamic GnRH neurons in an in vitro membrane-based model, BioFactors 47 (2021) 93–111, https://doi.org/10.1002/biof.1701.

[2] A. Piscioneri, S. Morelli, M. Mele, M. Canonaco, E. Bilotta, P. Pantano, E. Drioli, L. De Bartolo, Neuroprotective effect of human mesenchymal stem cells in a compartmentalized neuronal membrane system, Acta Biomater. 24 (2015) 297–308, https://doi.org/10.1016/j.actbio.2015.06.013.

[3] G. Giusi, R.M. Facciolo, M. Rende, R. Alo, A. Di Vito, S. Salerno, S. Morelli, L. De Bartolo, E. Drioli, M. Canonaco, Distinct α subunits of the GABAA receptor are responsible for early hippocampal silent neuron-related activities, Hippocampus 19 (2009) 1103–1114, https://doi.org/10.1016/j.neulet.2011.03.093.

[4] B. Memoli, S. Salerno, A. Procino, L. Postiglione, S. Morelli, M.L. Sirico, F. Giordano, M. Ricciardone, E. Drioli, V.E. Andreucci, L. De Bartolo, A translational approach to micro-inflammation in end-stage renal disease: molecular effects of low levels of interleukin-6, Clin. Sci. 119 (2010) 163–174, https://doi.org/10.1042/CS20090634.

[5] L. De Bartolo, S. Morelli, M. Rende, C. Campana, S. Salerno, N. Quintiero, E. Drioli, Human hepatocyte morphology and functions in a multibore fiber bioreactor, Macromol. Biosci. 7 (2007) 671–680, https://doi.org/10.1002/mabi.200600281.

[6] S. Morelli, S. Salerno, M. Rende, L.C. Lopez, P. Favia, A. Procino, B. Memoli, V. E. Andreucci, R. d'Agostino, E. Drioli, L. De Bartolo, Human hepatocyte functions in a galactosylated membrane bioreactor, J. Memb. Sci. 302 (2007) 27–35, https://doi.org/10.1016/j.memsci.2007.06.027.

[7] S.K. Aghdam, A.B. Khoshfetrat, R. Rahbarghazi, H. Jafarizadeh-Malmiri, M. Khaksar, Collagen modulates functional activity of hepatic cells inside alginate-galactosylated chitosan hydrogel microcapsules, Int. J. Biol. Macromol. 156 (2020) 1270–1278, https://doi.org/10.1016/j.ijbiomac.2019.11.164.

[8] O.M. Kolawole, W.M. Lau, V.V. Khutoryanskiy, Methacrylated chitosan as a polymer with enhanced mucoadhesive properties for transmucosal drug delivery, Int. J. Pharm. 550 (2018) 123–129, https://doi.org/10.1016/j.ijpharm.2018.08.034.

[9] U. D'Amora, A. Ronca, S. Scialla, A. Soriente, P. Manini, J.W. Phua, C. Ottenheim, A. Pezzella, G. Calabrese, M.G. Raucci, L. Ambrosio, Bioactive composite Methacrylated Gellan gum for 3D-printed bone tissue-engineered scaffolds, Nanomaterials 13 (2023) 772, https://doi.org/10.3390/nano13040772.

[10] M.A. Rahman, Collagen of extracellular matrix from marine invertebrates and its medical applications, Mar. Drugs 17 (2019) 118, https://doi.org/10.3390/md17020118.

[11] D. Coppola, C. Lauritano, F. Palma Esposito, G. Riccio, C. Rizzo, D. de Pascale, Fish waste: from problem to valuable resource, Mar. Drugs 19 (2) (2021) 116, https://doi.org/10.3390/md19020116.

[12] N.M.H. Khong, F.M. Yusoff, B. Jamilah, M. Basri, I. Maznah, K.W. Chan, N. Armania, J. Nishikawa, Improved collagen extraction from jellyfish (Acromitus hardenbergi) with increased physical-induced solubilization processes, Food Chem. 251 (2018) 41–50, https://doi.org/10.1016/j.foodchem.2017.12.083.

[13] D. Coppola, M. Oliviero, G.A. Vitale, C. Lauritano, I. D'Ambra, S. Iannace, D. de Pascale, Marine collagen from alternative and sustainable sources: extraction, processing and applications, Mar. Drugs 18 (4) (2020) 214, https://doi.org/10.3390/md18040214.

[14] E. Song, S. Yeon Kim, T. Chun, H.J. Byun, Y.M. Lee, Collagen scaffolds derived from a marine source and their biocompatibility, Biomaterials 27 (2006) 2951–2961, https://doi.org/10.1016/j.biomaterials.2006.01.015.

[15] L. Salvatore, N. Gallo, M.L. Natali, L. Campa, P. Lunetti, M. Madaghiele, F.S. Blasi, A. Corallo, L. Capobianco, A. Sannino, Marine collagen and its derivatives: versatile and sustainable bio-resources for healthcare, Mater. Sci. Eng. C Mater. Biol. Appl. 13 (2020) 110963, https://doi.org/10.1016/j.msec.2020.110963.

[16] S. Addad, J.Y. Exposito, C. Faye, S. Ricard-Blum, C. Lethias, Isolation, characterization and biological evaluation of jellyfish collagen for use in biomedical applications, Mar. Drugs 9 (6) (2011) 967–983, https://doi.org/10.3390/md9060967.

[17] H. Vieira, G.M. Lestre, R.G. Solstad, A.E. Cabral, A. Botelho, C. Helbig, D. Coppola, D. de Pascale, J. Robbens, K. Raes, et al., Current and expected trends for the marine chitin/chitosan and collagen value chains, Mar. Drugs 21 (12) (2023) 605, https://doi.org/10.3390/md21120605.

[18] I.P. Smith, M. Domingos, S.M. Richardson, J. Bella, Characterization of the biophysical properties and cell adhesion interactions of marine invertebrate collagen from Rhizostoma pulmo, Mar. Drugs 21 (2) (2023) 59, https://doi.org/10.3390/md21020059.

[19] S. Rabotyagova, Peggy Cebe, David L. Kapla, Collagen structural hierarchy and susceptibility to degradation by ultraviolet radiation, Mater. Sci. Eng. C 28 (2008) 1420–1429, https://doi.org/10.1016/j.msec.2008.03.012.

[20] F. Paradiso, J. Fitzgerald, S. Yao, F. Barry, F. Taraballi, D. Gonzalez, R.S. Conlan, L. Francis, Marine collagen substrates for 2D and 3D ovarian Cancer cell systems, Front. Bioeng. Biotechnol. 7 (2019) 343, https://doi.org/10.3389/fbioe.2019.00343.

[21] A. Sorushanova, L.M. Delgado, Z. Wu, N. Shologu, A. Kshirsagar, R. Raghunath, A. M. Mullen, Y. Bayon, A. Pandit, M. Raghunath, D.I. Zeugolis, The collagen Suprafamily: from biosynthesis to advanced biomaterial development, Adv. Mater. 31 (2019) 1801651, https://doi.org/10.1002/adma.201801651.

[22] F.F. Felician, R.H. Yu, M.Z. Li, C.J. Li, H.Q. Chen, Y. Jiang, T. Tang, W.Y. Qi, H. M. Xu, The wound healing potential of collagen peptides derived from the jellyfish rhopilema esculentum, Chin. J. Traumatol. 22 (2019) 12–20, https://doi.org/10.1016/j.cjtee.2018.10.004.

[23] T. Nagai, Characterization of acid-soluble collagen from skins of surf smelt (Hypomesus Pretiosus Japonicus Brevoort), FNS 01 (2010) 59–66, https://doi.org/10.4236/fns.2010.12010.

[24] J. Zhang, R. Duan, L. Huang, Y. Song, J.M. Regenstein, Characterisation of acid-soluble and pepsin-solubilised collagen from jellyfish (Cyanea Nozakii Kishinouye), Food Chem. 150 (2014) 22–26, https://doi.org/10.1016/j.foodchem.2013.10.116.

[25] H.S. Jeong, J. Venkatesan, S.K. Kim, Isolation and characterization of collagen from marine fish (Thunnus Obesus), Biotechnol. Bioproc. E 18 (2013) 1185–1191, https://doi.org/10.1007/s12257-013-0316-2.

[26] F. Zhang, A. Wang, Z. Li, S. He, L. Shao, Preparation and characterisation of collagen from freshwater fish scales, FNS 02 (08) (2011) 818–823, https://doi.org/10.4236/fns.2011.28112.

[27] C. Noè, M. Zanon, A. Arencibia, M.J. López-Muñoz, N. Fernández De Paz, P. Calza, M. Sangermano, UV-cured chitosan and gelatin hydrogels for the removal of As(V) and Pb(II) from water, Polymers 14 (2022) 1268, https://doi.org/10.3390/polym14061268.

[28] A. Piscioneri, S. Morelli, T. Ritacco, M. Giocondo, R. Peñaloza, E. Drioli, L. De Bartolo, Topographical cues of PLGA membranes modulate the behavior of hMSCs, myoblasts and neuronal cells, Colloids Surf. B Biointerfaces 222 (2023) 113070, https://doi.org/10.1016/j.colsurfb.2022.113070.

[29] S. Morelli, A. Piscioneri, E. Drioli, L. De Bartolo, Neuronal differentiation modulated by polymeric membrane properties, Cells Tissues Organs 204 (2017) 164–178, https://doi.org/10.1159/000477135.

[30] A. Martínez, M.D. Blancoa, N. Davidenkob, R.E. Cameron, Tailoring chitosan/collagen scaffolds for tissue engineering: effect of composition and different crosslinking agents on scaffold properties, Carbohydr. Polym. 132 (2015) 606–619, https://doi.org/10.1016/j.carbpol.2015.06.084.

[31] M. Raghavankutty, G.M. Jose, M. Sulaiman, G.M. Kurup, Evaluating the biocompatibility of marine-derived chitosan–collagen polymeric blends for biomedical applications, J. Bioact. Compat. Polym. 33 (2018) 439–455, https://doi.org/10.1177/0883911517747892.
[32] C. Correia, R.O. Sousa, A.C. Vale, D. Peixoto, T.H. Silva, R.L. Reis, I. Pashkuleva, N. M. Alves, Adhesive and biodegradable membranes made of sustainable catechol-functionalized marine collagen and chitosan, Colloids Surf. B Biointerfaces 213 (2022) 112409, https://doi.org/10.1016/j.colsurfb.2022.112409.
[33] K. Thongchai, P. Chuysinuan, T. Thanyacharoen, S. Techasakul, S. Ummartyotin, Integration of collagen into chitosan blend film composites: physicochemical property aspects for pharmaceutical materials, SN Appl. Sci. 2 (2020) 255, https://doi.org/10.1007/s42452-020-2052-5.
[34] A. Piscioneri, C. Campana, S. Salerno, S. Morelli, A. Bader, F. Giordano, E. Drioli, L. De Bartolo, Biodegradable and synthetic membranes for the expansion and functional differentiation of rat embryonic liver cells, Acta Biomater. 7 (2011) 171–179, https://doi.org/10.1016/j.actbio.2010.07.039.
[35] S. Salerno, A. Piscioneri, S. Morelli, M.B. Al-Fageeh, E. Drioli, L. De Bartolo, Membrane bioreactor for expansion and differentiation of embryonic liver cells, Ind. Eng. Chem. Res. 52 (2013) 10387–10395, https://doi.org/10.1021/ie400035d.
[36] C. Zhong, R. Zhuang, H. Xie, L. Zhou, X. Xu, S. Zheng, Hepatocyte growth factor-loaded collagen-chitosan scaffold containing differentiated bone marrow-derived mesenchymal stem cells as a model for hepatic tissue engineering, J. Biomat. Tissue Eng. 6 (2016) 621–628, https://doi.org/10.1166/jbt.2016.1478.
[37] B.Y. Yu, P.H. Chou, C.A. Chen, Y.M. Sun, S.S. Kung, C3A cell behaviors on micropatterned chitosan collagen gelatin membranes, J. Biomater. Appl. 22 (2007) 255–274, https://doi.org/10.1177/0885328207076780.
[38] D.N. Carvalho, M. Gelinsky, D.S. Williams, A. Mearns-Spragg, R.L. Reis, T.H. Silva, Marine collagen-chitosan-fucoidan/chondroitin sulfate cryo-biomaterials loaded with primary human cells envisaging cartilage tissue engineering, Int. J. Biol. Macromol. 241 (2023) 124510, https://doi.org/10.1016/j.ijbiomac.2023.124510.
[39] A. Zeigerer, A. Wuttke, G. Marsico, S. Seifert, Y. Kalaidzidis, M. Zerial, Functional properties of hepatocytes in vitro are correlated with cell polarity maintenance, Exp. Cell Res. 350 (2017) 242–252, https://doi.org/10.1016/j.yexcr.2016.11.027.
[40] Y. Zhao, S. Chen, J. Cai, Z. Song, J. Che, C. Liu, C. Wu, M. Ding, H. Deng, Derivation and characterization of hepatic progenitor cells from human embryonic stem cells, PloS One 4 (2009) e6468, https://doi.org/10.1371/journal.pone.0006468.